



Diversity of the *Ixodes ricinus* Microbiome Across Belgian Ecoregions and Its Association with Pathogen and Symbiont Presence

Camille Philippe^{1,2} · Lianet Abuin Denis^{3,4} · Manoj Fonville⁵ · Bert Devriendt² · François E. Dufrasne¹ · Dasiel Obregon⁶ · Apolline Maître³ · Štefánia Skičková⁷ · Eric Cox² · Hein Sprong⁵ · Alejandro Cabezas Cruz³ · Marcella Mori¹

Received: 9 April 2025 / Accepted: 15 June 2025
© The Author(s) 2025

Abstract

Ticks are important vectors of zoonotic pathogens, and their presence can be influenced by the composition of the tick microbiome. In turn, this microbiome is shaped by environmental and ecological factors, as demonstrated in several studies conducted under controlled conditions. However, the extent of these influences under natural ecological conditions remains underexplored. In this study, we investigated the diversity of the microbiome and the prevalence of pathogens in *Ixodes ricinus* nymphs across three distinct Belgian ecoregions: Sandy Loam, Condroz, and Ardennes. Using real-time quantitative PCR (qPCR) and Oxford Nanopore 16S rRNA sequencing, we assessed how geography and pathogen presence influence tick-associated microbial communities. Our results revealed significant regional differences in microbiome composition and pathogen prevalence. *Borrelia burgdorferi* sensu lato (s.l.) was most prevalent in the Ardennes (9% (7.4–10.9) vs 3.8% (2.8–5.2) in the Condroz and 2.1% (1.4–3.2) in Sandy Loam) while *Anaplasma phagocytophilum* was more common in the Sandy Loam region (21.1% (18.7–23.8) vs 4% (3–5.4) in the Condroz and 3.2% (2.2–4.4) in the Ardennes). Endosymbionts such as *Midichloria mitochondrii* and *Spiroplasma ixodetis* also exhibited distinct geographic distributions. Network analysis identified potential pathogen-microbiota interactions, with certain bacterial taxa showing positive or negative associations with specific pathogens. Moreover, microbiome composition was influenced not only by ecoregion but also by microorganisms such as *Rickettsia helvetica*, suggesting that its colonization may actively shape microbial community structure, potentially through competition or facilitation mechanisms. Additionally, microbiome network robustness varied across ecoregions, highlighting the role of ecological context in shaping microbial interactions within ticks. These findings underscore the complex interplay between geography, pathogen presence, and microbial diversity in ticks, highlighting the importance of integrating these interactions to inform microbiome-based strategies for vector control and disease prevention.

Keywords Tick microbiome · Pathogen-symbiont-microbiota interactions · Ecoregions · *Ixodes ricinus* · Nymph sex

✉ Marcella Mori
Marcella.Mori@sciensano.be

¹ Sciensano, Belgian Institute for Health, Brussels, Belgium

² Laboratory of Immunology, Department of Translational Physiology, Infectiology and Public Health, Faculty of Veterinary Medicine, Ghent University, Merelbeke, Belgium

³ Anses, INRAE, Ecole Nationale Vétérinaire d'Alfort, UMR BIPAR, Laboratoire de Santé Animale, Maisons Alfort, France

⁴ Animal Biotechnology Department, Centre for Genetic Engineering and Biotechnology, Havana, Cuba

⁵ Centre for Infectious Disease Control, National Institute for Public Health and Environment (RIVM), Bilthoven, Netherlands

⁶ School of Environmental Sciences, University of Guelph, Guelph, ON, Canada

⁷ Department of Animal Physiology, Faculty of Science, Institute of Biology and Ecology, Pavol Jozef Šafárik University in Košice, Košice, Slovakia

Introduction

Ticks are among the most significant arthropod vectors of zoonotic pathogens, transmitting a wide range of bacteria, viruses, and protozoa that cause disease in humans and animals [1]. In addition to harboring pathogens, ticks also maintain a diverse microbiome composed of commensals [2–4] and symbionts [5], which may play a critical role in shaping pathogen colonization [6–8] and vector competence [9]. While laboratory-based studies have demonstrated that both environmental factors such as temperature [10, 11] and pathogen presence [8, 12] can shape the tick microbiome, the extent of these interactions under natural ecological conditions remains poorly understood.

The microbiome of *Ixodes ricinus*, one of the most widespread tick species in Europe, is known to vary based on tick developmental stage, habitat characteristics, and host feeding history [2–4]. Previous research has suggested that ecological differences, such as climate [13] or wildlife reservoirs [14], influence the microbiota of *Ixodes* populations, potentially modulating pathogen occurrence and aspects of tick biology. Moreover, certain endosymbionts, such as *Midichloria mitochondrii* [15] and *Spiroplasma* sp. [16] may play a role in shaping the tick microbiome and modulating pathogen dynamics.

Recent studies further illustrate that microbial community structure and diversity in ticks can be strongly influenced by geographic factors. For example, elevational gradients have been linked to decreases in phylogenetic microbial alpha diversity within tick bacterial communities, indicating that higher altitudes may reduce microbiome complexity [17]. Additionally, analyses of *Ixodes* ticks from different regions in the eastern part of the USA have revealed that microbiome composition varies significantly with geographic location, as well as by tick species and sex [18]. These findings underscore the importance of environmental and biological factors in shaping the microbiome landscape of ticks across diverse habitats.

While the microbiome might influence pathogen ecology, recent studies have also demonstrated that tick-borne pathogens can actively reshape microbiome composition revealing a bidirectional relationship with coexisting resident microbial communities [12, 19, 20]. For instance, *Rickettsia helvetica* presence is associated with a reduction in microbiome diversity and microbial interactions in *I. ricinus* [20], suggesting that certain pathogens may outcompete commensal taxa. Network analysis has revealed that the presence of *R. helvetica* reduces microbiome connectivity [20], limiting microbial co-occurrence and potentially altering functional metabolic pathways. Similarly, pathogen presence has been linked to shifts in microbial community structure, as seen with *Borrelia* and

Anaplasma, which subvert microbial networks in *I. ricinus* [13]. However, the extent to which these interactions vary across different ecological contexts remains unclear. Elucidating these dynamics is essential to understand influence on vector competence and other physiological processes relevant to tick fitness.

Belgium's diverse ecoregions provide an ideal natural setting to explore these interactions. The country encompasses distinct ecological zones ranging from the lowland Sandy Loam region, the transitional Condroz region, to the forested Ardennes. Each of these ecoregions presents unique soil compositions, vegetation types, and host availability [21, 22], all of which could contribute to differences in tick microbiome diversity and pathogen prevalence. These environmental differences provide a unique opportunity to investigate how geography shapes the dynamics of tick-borne pathogen occurrence, microbiome diversity, and vector ecology.

In this study, we investigated the microbiome composition and pathogen prevalence of *I. ricinus* nymphs collected from three Belgian ecoregions, with a specific focus on how microbiome variation shaped by geography, pathogen, and symbiont presence influences microbial community structure. We employed real-time quantitative PCR (qPCR) to assess pathogen and symbiont prevalence and Oxford Nanopore Technologies (ONT) 16S rRNA sequencing to characterize microbial diversity. We further explored potential interactions between specific pathogens and microbiota. Additionally, we analyzed microbial co-occurrence networks to assess whether microbial interactions differed between ecoregions and how robust these networks were to ecological variation.

Our comprehensive analyses revealed that the local ecological context not only influenced the prevalence of key pathogens and symbionts in *I. ricinus* but also profoundly shaped the architecture of their microbial communities. The marked regional differences in tick sex distribution, pathogen occurrence (including notable shifts in agents such as *B. burgdorferi* s.l., *A. phagocytophilum*, *Babesia* spp., and *Neoehrlichia mikurensis*), and the unique, robust co-occurrence networks—particularly in the Sandy Loam ecoregion—underscored a complex interplay between environmental factors and microbial dynamics. These findings highlight ecological heterogeneity as a key driver of vector competence and potentially pathogen transmission, emphasizing the need to integrate environmental and microbial network perspectives into predictive models and innovative strategies for tick-borne disease control.

Materials and Methods

Tick Sampling

Three ecoregions with highly diverse ecological, vegetation, and soil compositions in Belgium were selected for

sampling: the Sandy Loam (lowland of the Flemish Valley), the Condroz (south of the River Meuse and a transition area between Ardennes and the lying region of the country), and the Ardennes (the southern, hilly, forested region of Wallonia). Within each ecoregion, two sites were chosen for tick sampling: Het Leen (51°10'00.1" N 3°34'17.6" E) and Bellebargiebos (51°10'09.8" N 3°37'43.5" E) in Sandy Loam, Bois d'Hony (50°32'55.4" N 5°34'36.1" E) and Bois de la Famelette (50°33'29.6" N 5°33'07.1" E) in Condroz, and Faux-Mayaux (49°59'10.1" N 5°11'16.7" E) and Bois Tibaut (49°54'45.8" N 5°07'04.0" E) in the Ardennes (Fig. 1A). *Ixodes ricinus* ticks were collected on flannel cloths using the flagging method between April and October 2023, then transported to the laboratory and stored at -20°C until analysis (the entire analytic workflow is depicted in Fig. 1B). A minimum of 500 ticks per site were collected. Except for ticks used for real-time quantitative PCR (qPCR) validation, only nymphal ticks were included in this study.

Tick Homogenization, Pathogen Detection, and Sex Determination by qPCR

After thawing at room temperature, individual ticks were morphologically identified to species and then washed in 70% ethanol for 2 min, followed by two rinses of 2 min in nuclease-free water. Ticks were then transferred into a tube containing 310 μL of sterile PBS and two metallic 5-mm beads (69,989, Qiagen®, Aarhus, Denmark) and

homogenized by beating at 25 Hz for 5 min using a tissue lyser (85300, Qiagen®, Aarhus, Denmark). Ten microliters of the homogenate were heated at 95°C for 5 min, centrifuged, and then diluted 1:10 in sterile milliQ water. The extracted material was preserved at -20°C until further analysis. All qPCRs were carried out directly on the heat-inactivated diluted homogenates. This method was validated using positive tick homogenates characterized in previous studies [24]. qPCR for *B. burgdorferi* (s.l.), *B. miyamotoi*, *A. phagocytophilum*, *Babesia* spp., *R. helvetica*, *N. mikurensis*, *S. ixodetis*, *M. mitochondrii*, and *Rickettsiella* was run on a LightCycler® 480 (Roche Diagnostics Nederland B.V, Almere, the Netherlands) with exact primers/probes combinations and conditions as formerly described [24, 25]. The internal control consisted of amplification of the 16S rRNA fragment as described elsewhere [25].

In addition, we used a novel qPCR to identify the nymph sex, characterizing them either as male or female ticks [26]. Primers were designed from *I. ricinus* male-specific genomic sequence (PP216546.1). Reaction conditions were conducted in a final volume of 20 μL using iQ multiplex 2x-Powermix (Bio-Rad, Belgium), primers MV192-F51 (5'-AGGAGACGAACATAATGGTA-3') and MV192-R171 (5'-TCATTATTGCGAACATTTTCTG-3') at 200 nM each, probe MV192-P115 (5'-ATTO425-TCCTTCGCCGTCCTTTCTAATGGG-BHQ1-3') at 100 nM and 5 μL of tick's extract. The test was validated using adult ticks, and the sensitivity and specificity were 90% and 100%, respectively

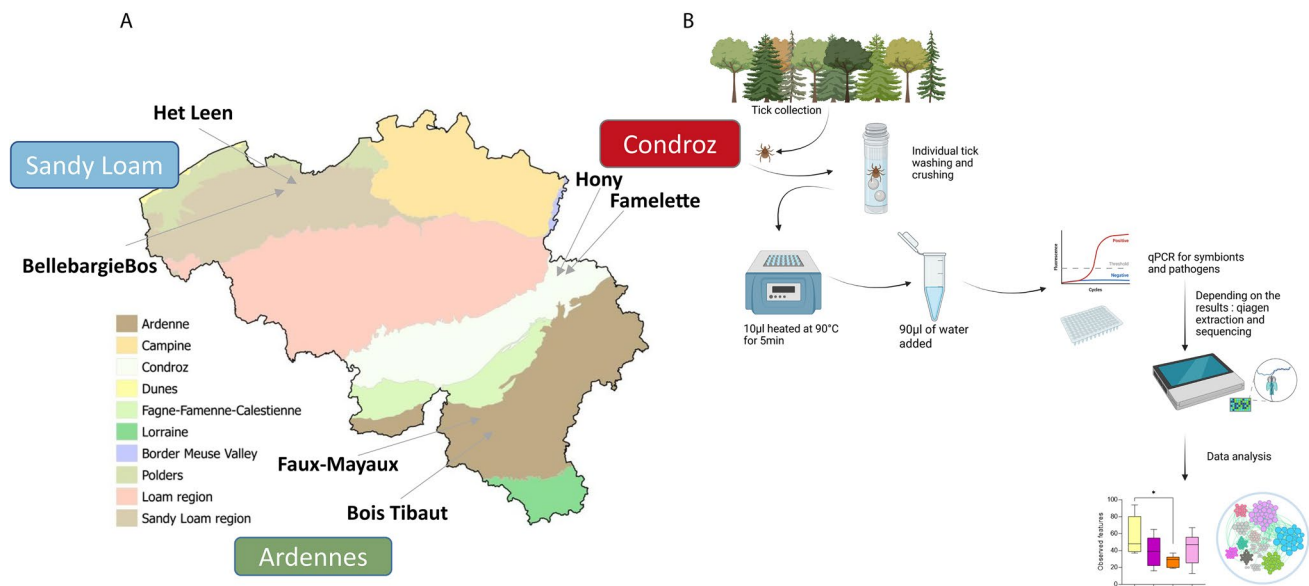


Fig. 1 Map of Belgian ecoregions indicating collection sites and workflow of tick collection and processing. **A** Ticks were collected from three distinct ecoregions in Belgium: Sandy Loam, Condroz, and Ardennes. Sampling sites included Het Leen, Bellebargiebos (Sandy Loam); Hony, Famelette (Condroz); and Bois Tibaut, Faux-Mayaux (Ardennes). Map adapted from [23]. **B** Questing *Ixodes*

ricinus nymphs were collected using the flagging method. Collected ticks were individually processed for DNA extraction, followed by pathogen screening via qPCR and microbiome analysis using Oxford Nanopore 16S rRNA sequencing. Data were analyzed to assess regional variations in microbiome composition, pathogen prevalence, and microbial interactions

[26]. Cycling conditions included a step at 95 °C for 5 min, followed by 55 cycles of a 5-s denaturation at 95 °C followed by a 35-s annealing-extension step at 60 °C and a final cooling cycle of 37 °C for 20 s. We tested the qPCR assay in our settings using 41 adult males and 6 adult females derived from Sciensano's tick collection (Fig. S1).

The entire sample processing, from homogenate to qPCR to sequencing, was controlled by parallel processing of samples consisting of PBS only.

Statistical analyses of the qPCR results were conducted in R 4.2.1 [27]. Pearson's chi-squared tests or Fisher's exact tests, as appropriate, were used to compare pathogen prevalence across ecoregions ($p < 0.01$) using p values < 0.01 as considered significant. Associations between pathogens, symbionts, and nymph sex were calculated with Yule's Q in R Studio, using a $p < 0.05$ and a threshold of 0.3. Networks were visualized using Gephi.

DNA Extraction and 16S rRNA Oxford Nanopore Sequencing

Twenty ticks per site were selected for 16S-amplified Nanopore sequencing. Depending on sample availability, the chosen strategy was as follows: three female and three male (as defined by sex-qPCR) *S. ixodetis*-positive nymphs, eight females *B. burgdorferi* (s.l.)-positive nymphs, three females *R. helvetica*-positive, and three females *A. phagocytophilum*-positive nymphs. DNA was extracted from 100 µL of the initial homogenized material using the Qiagen extraction, following the manufacturer's instructions. Prior to sequencing, DNA samples were re-tested by qPCR to confirm positivity for the selected pathogen/symbiont, and only those samples reconfirmed as positive were employed for further steps. Whole 16S fragment (1500 bp) was amplified by conventional PCR using universal primers 27F (5'-AGAGTTTGATCCTGGCTCAG-3') and 1541R (5'-AAGGAGGTGATCCAGCCGCA-3') [28].

Reaction conditions were conducted in a final volume of 25 µL using LongAmp™ Taq 2X Master Mix (New England Biolabs, MA, USA), primers at 400 nM each, and 3 µL DNA. Run cycles consisted of an initial denaturation step at 94 °C for 30 s followed by 30 cycles of amplification, consisting of denaturation at 94 °C for 20 s, annealing at 56 °C for 40 s, extension at 65 °C for 75 s, and a final extension step at 65 °C for 10 min. Amplicons were visualized on a GelRed Nucleic Acid Stained 2% agarose gel, and if visible, they were used for sequencing. Oxford Nanopore sequencing was realized with the MinIon Mk1C device and run on R10.4.1 flow cells. Native barcoding kit (SQK-NBD114.24) allowing the sequencing of the 1500 bp 16S fragment in samples was used according to the manufacturer's protocol. The Minion was running for 48 h; reads smaller than 200 bp were not considered.

Per site, 20 samples were sequenced (120 in total), together with 6 negative control samples, which were processed similarly and contained only the 2 beads and PBS.

Sequence Processing, Taxonomic Classification, and Removal of Contaminants

The 16S rRNA sequences resulting from ONT run were processed using the EPI2ME 16S Workflow in EPI2ME labs software (<https://github.com/epi2me-labs/wf-16s>), with Minimap2 for alignment and the SILVA database (SILVA_138_1) [27] for taxonomic classification (definition of operational taxonomic units-OTU). The taxonomic table, constructed at the genus resolution level, was created using default settings, with memory set to 8 GB in the Nextflow configuration. Operational taxonomic units rarefaction curves were split into two graphs in R [29] to assess sequencing depth and evaluate true diversity (Fig. S2 A, B).

The list of taxa (Table S2) was filtered for contaminants using the Decontam package [30] in R [29], with a probability threshold of 0.5 to identify and remove potential spurious reads using the "prevalence" method. This approach compares the prevalence of each sequence feature in true samples against its prevalence in negative controls, allowing for the identification and removal of contaminants. In addition, taxa with fewer than three reads in any sample were excluded to focus on relevant microorganisms. This resulted in a total of 395 OTUs for downstream analyses (Table S3 and S4).

Diversity and Differential Taxonomic Composition Analysis

Alpha diversity metrics were calculated in Qiime2 using the q2-diversity plugin, with the Kruskal–Wallis test ($p \leq 0.05$). Results were imported into GraphPad Prism version 9.4.1 (681) (GraphPad Software Inc.) to generate graphs. Observed features (number of taxa) were used to assess alpha diversity. The Bray–Curtis dissimilarity index was employed to evaluate compositional differences, with comparison based on a PERMANOVA test ($p < 0.05$). In addition, the Bray–Curtis index was also explored with Betadisper function from the Vegan R package [31] in R [29] to analyze differences in dispersion within sample groups, with the ANOVA test ($p < 0.05$).

To assess differences in taxonomic composition between sample groups, we utilized the ANOVA-Like Differential Expression (ALDEx2) package [32] implemented in R [29]. This method applies a centered log-ratio (clr) transformation to appropriately handle compositional data, incorporates Monte Carlo sampling to estimate posterior distributions of clr-transformed values, and employs the Kruskal–Wallis test for statistical comparisons, providing a robust framework for

differential abundance analysis. Visualization of significant taxa ($p < 0.05$) was performed as heatmaps, generated using the heatmap.2 function in R [29]. The Jaccard distance calculated in R [29] using the Vegan package [31] was used to compare taxonomic composition between samples, highlighting differences based on species presence or absence.

Network Analysis and Microbial Associations

Networks were generated in R [27] using a Sparse Correlations for Compositional data (SparCC) method [33] with a cutoff of > 0.3 for positive correlations and < -0.30 for negative correlations and visualized in Gephi 0.10.1. A detailed description of the nodes and edges has been outlined previously [34]. Briefly, in these networks, a taxon is represented by a node, and colored edges connect the nodes depending on their positive (green) or negative (red) correlation.

The network comparisons and Jaccard index were conducted using the package Network Construction and Comparison for Microbiome Data (NetCoMi) [35] in R [29], with a cutoff of 0.5. Jaccard index is the measure of similarity of the most central nodes between two networks. A Jaccard index of 1 indicates complete similarity between networks while a Jaccard index of 0 means no similarity.

The local connectivity of *Anaplasma*, *Borrelia*, *Spiroplasma*, and *Rickettsia* within the ecoregion networks was investigated by identifying the nodes to which these taxa were connected. Network robustness was analyzed by assessing the impact of adding or removing nodes to the network. For the node removal robustness analysis, the Network Strengths and Weaknesses Analysis (NetSwan) package [36] was used in R [27]. Betweenness centrality, degree centrality, and cascading were the strategies used to estimate the proportion of nodes that needed to be removed to achieve a connectivity loss of 0.80. For the node addition robustness analysis, a previously described method was used [37]. In this method, nodes were randomly added to the networks, and the size of the largest connected component (LCC) and the average path length (APL) were calculated in R [27]. Different numbers of nodes were gradually added: 100, 200, 300, 400, and 500. Unique or shared taxa across ecoregion networks were visualized with Venn diagrams generated using the Venn webtool (<https://bioinformatics.psb.ugent.be/webtools/Venn/>).

Results

Sex-Linked Patterns, Pathogen Occurrence, and Microorganism Associations Vary Across Ecoregions

In total, 3072 *I. ricinus* nymphs were collected: 1008 from the Sandy Loam region (503 from Het Leen and 505 from

Bellebargiebos), 1050 from the Condroz region (540 from bois de Hony and 510 from bois de la Famelette), and 1014 from the Ardennes region (504 from Bois Tibaut and 510 from Faux-Mayaux).

Real-time qPCR assays that determined whether nymphs would molt into male or female adult ticks revealed significant differences in tick sex ratios across ecoregions. The proportion of males was significantly lower in Sandy Loam (37.9%, 95% CI 35–40.9%) compared to Condroz (44.6%, 95% CI 41.6–47.6%) and the Ardennes (44.8%, 95% CI 41.7–47.8%) ($p < 0.005$) (Fig. 2A and Table S1).

Differences in prevalence were observed for all pathogens and symbionts across ecoregions, with the exception of *R. helvetica*, which showed a similar prevalence range (4.8–5.8%) across regions (Fig. 2B and Table S1). The prevalence of *A. phagocytophilum* was significantly higher in Sandy Loam (2.2%, 95% CI 1.4–3.3%) compared to Condroz (0.8%, 95% CI 0.4–1.5%) ($p < 0.01$), though it did not differ significantly from that in the Ardennes (1%, 95% CI 0.5–1.8%). *Babesia* spp. were significantly more prevalent in Condroz (3.2%, 95% CI 2.3–4.5%) than in the Ardennes (1.5%, 95% CI 0.9–2.4%) ($p < 0.01$). Additionally, *B. burgdorferi* s.l. prevalence was highest in the Ardennes (9%, 95% CI 7.4–10.9%), compared to Condroz (3.8%, 95% CI 2.8–5.2%) and Sandy Loam (2.1%, 95% CI 1.4–3.2%) ($p < 0.01$). *B. miyamotoi* prevalence was significantly higher in Condroz (1.1%, 95% CI 0.7–2%) than in the Ardennes (0.3%, 95% CI 0.1–0.9%) ($p < 0.02$), and *N. mikurensis* was absent in Sandy Loam but was more prevalent in Condroz (1.9%, 95% CI 1.2–2.9%) than in the Ardennes (0.2%, 95% CI 0–0.8%) ($p < 0.01$).

The prevalence of known endosymbionts also varied across ecoregions (Fig. 2C and Table S1). *M. mitochondrii* prevalence was significantly higher in the Ardennes (31.9%, 95% CI 29.1–34.8%) than in Condroz (17.3%, 95% CI 15.2–19.7%) and Sandy Loam (20.9%, 95% CI 18.5–23.6%) ($p < 0.01$). *Rickettsiella* was observed at a lower overall prevalence, being more common in Sandy Loam (2.7%, 95% CI 1.8–3.9%) than in Condroz (0.8%, 95% CI 0.4–1.5%) or the Ardennes (0.2%, 95% CI 0–0.8%) ($p < 0.01$). Furthermore, *S. ixodetis* prevalence was highest in Sandy Loam (21.1%, 95% CI 18.7–23.8%), exceeding its prevalence in both Condroz (4%, 95% CI 3–5.4%) and the Ardennes (3.2%, 95% CI 2.2–4.4%) ($p < 0.01$).

Association networks generated by Yule's Q calculations (Fig. 2D) revealed consistent patterns across ecoregions. In all regions, a positive association was observed between the female sex and *M. mitochondrii*, with a corresponding negative association between the male sex and *M. mitochondrii*. In Sandy Loam, a positive association was detected between *A. phagocytophilum* and *M. mitochondrii*, along with a negative association between *R. helvetica* and *S. ixodetis*. In Condroz, a positive association emerged

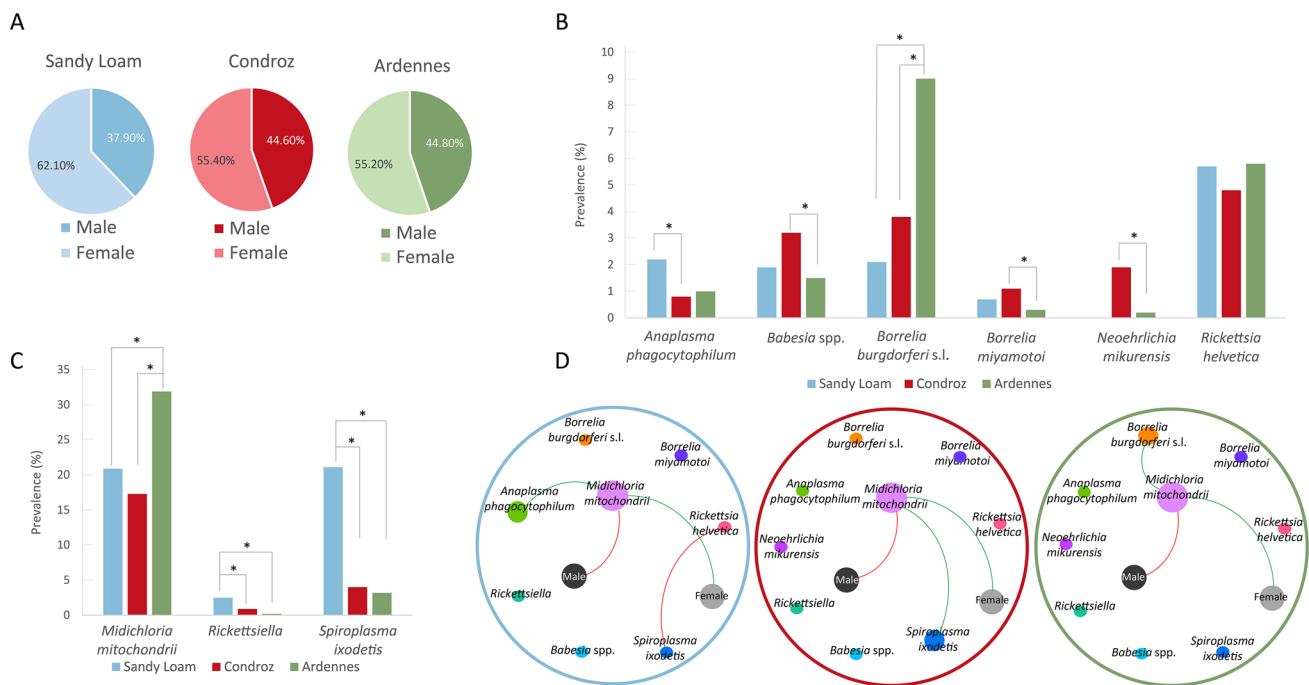


Fig. 2 Nymph sex distribution, pathogen, and endosymbiont prevalence across Belgian ecoregions. **A** Nymph sex distribution across the three ecoregions (Sandy Loam, Condroz, and Ardennes), showing the proportion of males and females in each region. **B** Pathogen prevalence in each ecoregion, including *B. burgdorferi* s.l., *B. miyamotoi*, *A. phagocytophilum*, *N. mikurensis*, *Babesia* spp., and *R. helvetica*. Asterisks (*) indicate statistically significant differences ($p < 0.01$) between ecoregions. **C** Endosymbiont prevalence across ecoregions,

including *M. mitochondrii*, *Rickettsiella*, and *S. ixodetis*. Asterisks (*) indicate statistically significant differences ($p < 0.02$). **D** Association network analysis between nymph gender, pathogen, and endosymbiont proportions. Associations were calculated using Yule's Q in R Studio, with a threshold of 0.3 and $p = 0.05$. Positive associations are represented by green lines, while negative associations are shown in red

between *M. mitochondrii* and *S. ixodetis*, whereas in the Ardennes, *B. burgdorferi* s.l. was positively associated with *M. mitochondrii*.

Tick Microbiome Composition Is Shaped by Ecoregion and *R. helvetica* Presence

Across the three ecoregions, we sequenced 120 nymph ticks (40 ticks per ecoregion) using ONT, generating over 50 GB of data. Sequencing depth was sufficient to capture microbial diversity, as indicated by rarefaction curves reaching a plateau at $\sim 10^5$ reads (Fig. S2A,B). Dominant taxa, characterized by the highest read counts across samples, included *Rickettsia*, *Arsenophonus*, *Methylocella*, and *Bradyrhizobium*.

Alpha diversity, assessed by the number of observed features, was used to evaluate within-sample OTU richness in relation to the presence of specific microorganisms as determined by qPCR. We focused on *A. phagocytophilum*, *B. burgdorferi* s.l., *R. helvetica*, and *S. ixodetis* due to their higher prevalence. In the Sandy Loam region, ticks positive for *A. phagocytophilum* exhibited significantly higher diversity than those positive for *R. helvetica* (Kruskal–Wallis,

$p < 0.01$, Fig. 3A), while no significant differences were detected among the other groups. In Condroz, the microbiome of ticks positive for *A. phagocytophilum* displayed a higher level of observed features compared to ticks positive for *B. burgdorferi* s.l. (Kruskal–Wallis, $p < 0.05$, Fig. 3A) and *R. helvetica* (Kruskal–Wallis, $p < 0.05$, Fig. 3A). In the Ardennes region, significant differences were observed between *S. ixodetis*-positive ticks and all the other pathogen-positive groups (Kruskal–Wallis, $p < 0.01$, Fig. 3A).

Beta diversity analyses using the Bray–Curtis index confirmed that community composition differed significantly among the three ecoregions (PERMANOVA, $F = 3.844$, $p = 0.0001$). Principal coordinates analysis (PCoA) based on these distances revealed that ticks from the Ardennes displayed a wider spread along both axes compared to those from Condroz and Sandy Loam, indicating a more heterogeneous microbial community (Fig. 3B).

Differential taxonomic analysis further demonstrated distinct microbial profiles in each ecoregion across conditions, although *Comamonas* and *Leptothrix* were consistently detected across all regions (Fig. 3C). Four taxa in ticks from the Sandy Loam region, 11 taxa in those from Condroz,

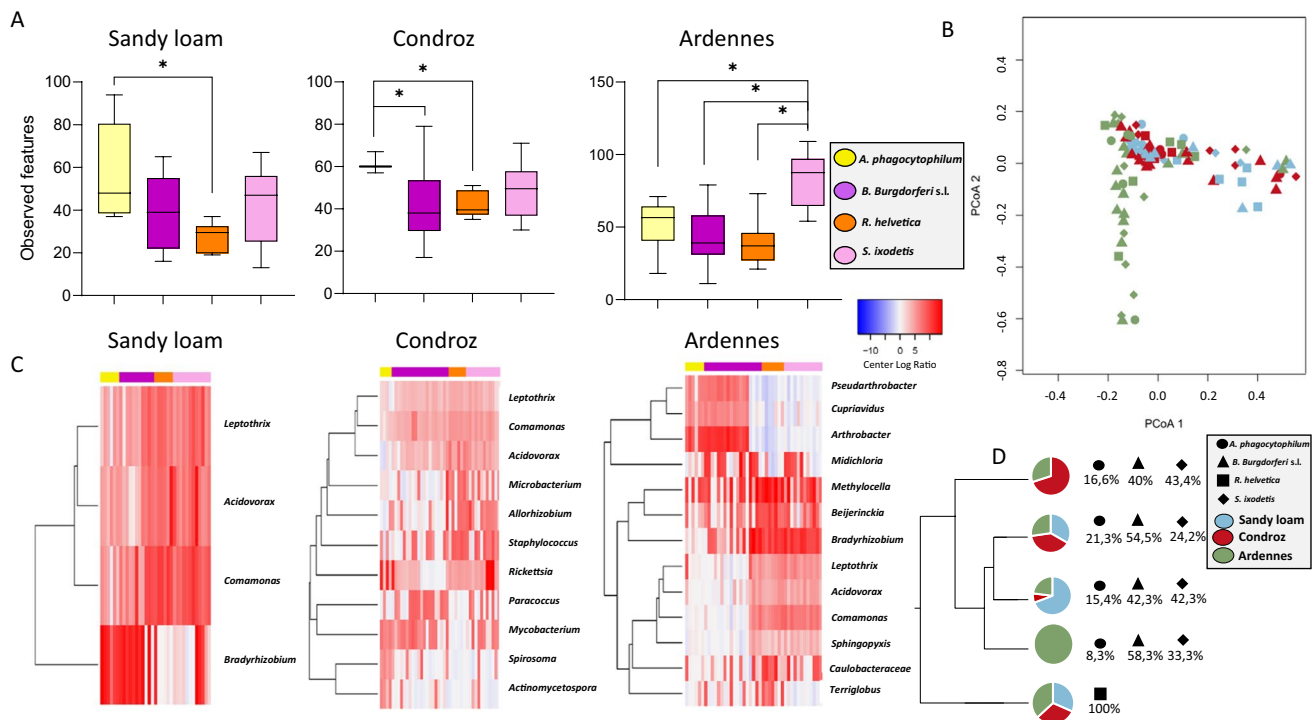


Fig. 3 Tick microbiome composition across ecoregions and in response to specific microorganisms. **A** Alpha diversity comparison of tick microbiomes across ecoregions (Sandy Loam, Condroz, and Ardennes) based on observed features. Kruskal–Wallis tests were performed for each ecoregion (Sandy Loam: $p=0.076$; Condroz: $p=0.085$; Ardennes: $p=0.006$). Asterisks (*) indicate statistical significance. **B** Beta diversity analysis using the Bray–Curtis dissimilarity index to compare microbial composition between ecoregions and in the presence of specific microorganisms (*A. phagocytophilum*, *B. burgdorferi* s.l., *R. helvetica*, *S. ixodetis*). A PERMANOVA test

demonstrated significant differences in beta dispersion among sample groups ($p=0.0001$). **C** Heatmap visualization of microbial taxa abundance across ecoregions and conditions. The heatmap was generated with heatmap.2 in R, using a red-to-blue gradient (red=high, blue=low). Values are clr-transformed relative abundances; colors therefore represent relative taxon representation, not absolute bacterial loads (see Methods). **D** Hierarchical clustering dendrogram of tick microbiome samples, showing grouping patterns based on ecoregion and the presence of particular microorganisms (*A. phagocytophilum*, *B. burgdorferi* s.l., *R. helvetica*, *S. ixodetis*)

and 13 taxa in ticks from the Ardennes were significantly associated with the presence of specific microorganisms. Moreover, analysis of Jaccard distances showed that *R. helvetica*-positive ticks clustered together regardless of ecoregion, suggesting a distinct microbiome signature linked to *R. helvetica* infection (Fig. 3D). In contrast, when considering the remaining ticks, one cluster containing individuals from all ecoregions emerged alongside three additional clusters that grouped ticks by their ecoregion. Notably, one branch comprised solely ticks from the Ardennes, underscoring the strong influence of geographic origin on microbiome composition.

Co-occurrence Network Analysis and Robustness Indicate Changes in Network Composition Depending on the Ecoregion

Modules networks (Fig. 4A) and topological features (Table 1) revealed that, across all ecoregions, positive microbial interactions were more common than negative

ones. This trend was especially pronounced in the Sandy Loam network, which exhibited a higher number of positive edges compared to the Condroz and Ardennes networks. In contrast, the Condroz network showed no negative interactions, and only one negative edge was detected in the Sandy Loam network, whereas the Ardennes network had the highest number of negative edges suggesting that the Ardennes had a competitive structure compared to the other networks. The Sandy Loam network also harbored the largest number of nodes, indicating that this was the more connected network, displaying approximately twice as many edges as the Condroz and Ardennes networks. This enhanced connectivity was supported by its smallest network diameter and as well as the highest average and weighted degrees. In contrast, the Condroz and Ardennes networks had fewer connections per node and a lower average degree. Condroz exhibited the highest modularity, indicating a more distinct community structure with more separate groups of taxa, supported by the fewest number of modules. The Sandy Loam and Ardennes

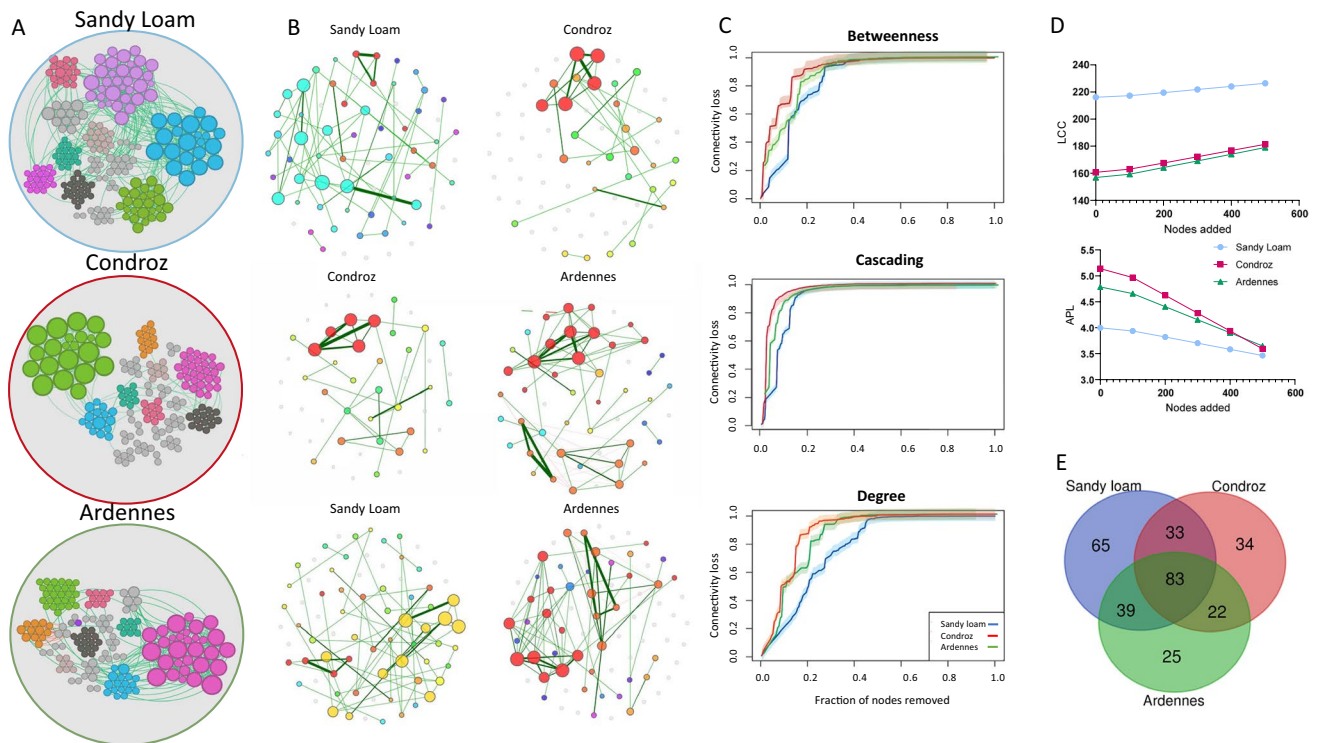


Fig. 4 Network analysis and robustness across ecoregions. **A** Module networks for each ecoregion (Sandy Loam, Condroz, and Ardennes), with modules shared across ecoregions represented in the same color. Positive interactions are shown in green, and negative interactions are shown in red. **B** Pairwise correlation networks (SparCC > 0.5 or < -0.5), illustrating microbial associations within each ecoregion. **C** Robustness analysis to node removal, measuring the stability of

microbial networks in each ecoregion when nodes are sequentially deleted. **D** Robustness analysis to node addition, showing changes in largest connected component (LCC) and average path length (APL) as new nodes are introduced into the network. **E** Venn diagram of shared nodes between ecoregions, depicting the overlap in microbial taxa across Sandy Loam, Condroz, and Ardennes.

Table 1 Topological features of the taxonomic network of each ecoregion

Network features	Sandy Loam	Condroz	Ardennes
Number of nodes	220	172	169
Number of edges	798	384	397
Positive interactions	797 (99.87%)	384 (100%)	379 (95.47%)
Negative interactions	1 (0.13%)	0 (0%)	18 (4.53%)
Modularity	0.722	0.762	0.678
Network diameter	12	19	14
Average degree	7.255	4.465	4.698
Weighted degree	2.745	1.672	1.646
Clustering coefficient	0.536	0.541	0.483
Number of modules	16	21	20

networks had shorter diameters, suggesting more efficient connectivity (Table 1).

Local connectivity of the microbes within the networks revealed that all four taxa (*Anaplasma*, *Borrelia*, *Rickettsia*, and *Spiroplasma*) were found in Sandy Loam. *Anaplasma* showed the largest connectivity among the four,

with connections with other 16 taxa. In the Condroz, only *Spiroplasma* was found in the network, and it was connected to four other taxa. In the Ardennes, *Borrelia* and *Rickettsia* were found, with *Borrelia* connected to four taxa and *Rickettsia* to one (Fig. S3 and Table 2). Comparison of nodes within the three major modules S1, S2, and S3 for Sandy Loam; C1, C2, and C3 for Condroz; and A1, A2, and A3 for the Ardennes revealed sharing of taxa among the different ecoregions (Fig. S4 and Table 3). S3, C1, C2, A1, and A2 were common modules across ecoregions, while the additional C3 and A3 modules were shared between Condroz and the Ardennes, highlighting the high similarity between these two ecoregions, as also observed in the network analysis structure (Fig. S4 and Table 2). Interestingly, in the Sandy Loam network, were all four taxa were found, *Anaplasma* was present in the second largest module S2 and *Rickettsia* and *Spiroplasma* were placed in the same module.

Pairwise correlation networks comparing ecoregions further underscored these differences, with the Condroz and Ardennes networks exhibiting similar structures, while the Sandy Loam network appeared distinct from the others (Fig. 4B). The Jaccard index confirmed these findings, as the

Table 2 Local connectivity of microbes found in each ecoregion network

Sandy Loam		Condroz		Ardennes	
<i>Anaplasma</i>	<i>Intrasporangiaceae</i>	<i>Spiroplasma</i>	<i>Tianweitzania</i>	<i>Borrelia</i>	<i>Candidatus Midichloria</i>
	<i>Schumannella</i>		<i>Fusobacterium</i>		<i>Kineococcus</i>
	<i>Conexibacter</i>		<i>Candidatus Nostocoida</i>		<i>Klenkia</i>
	<i>Enterococcus</i>		<i>Xanthomonadaceae</i>		<i>Pseudorhodofex</i>
	<i>Gemmataceae</i>				
	<i>Ilumatobacteraceae</i>			<i>Rickettsia</i>	<i>Gemmataceae</i>
	<i>Amaricoccus</i>				
	<i>Micromonospora</i>				
	<i>Sphingorhabdus</i>				
	<i>Asticcacaulis</i>				
	<i>Ellin6067</i>				
	<i>Haliangium</i>				
	<i>Verrucomicrobiaceae</i>				
	<i>Cnuibacter</i>				
	<i>Micromonosporaceae</i>				
<i>Borrelia</i>	<i>Conyzicola</i>				
<i>Rickettsia</i>	<i>Acetobacteraceae</i>				
	<i>Dokdonella</i>				
<i>Spiroplasma</i>	Unclassified				

Table 3 The percentage of taxa shared between different modules

	S1	S2	S3	C1	C2	C3	A1	A2	A3
S1	100	0%	0%	0%	2.50%	8.70%	0%	0%	3.85%
S2	0%	100%	0%	1.92%	0%	2.38%	0%	1.96%	0%
S3			100%	6.25%	10.41%	3.70%	10%	1.58%	8.33%
C1				100%	0%	0%	10.41%	34.42%	0%
C2					100%	0%	9.37%	0%	7.14%
C3						100%	2.63%	0%	10.41%
A1							100%	0%	0%
A2								100%	0%
A3									100%

Condroz-Ardennes network comparison showed the highest Jaccard index for degree, betweenness centrality, closeness centrality, and hub taxa (Table S1-3).

Robustness analyses provided additional insights in network structure: the Sandy Loam network was the most resilient to node removal, requiring a greater number of nodes to be removed before connectivity was compromised, whereas the Condroz network was the most vulnerable (Fig. 4C). In terms of robustness to node addition, the Sandy Loam network maintained the largest connected component (LCC) and a lower average path length (APL) compared to the other regions (Fig. 4D). The compositional analysis revealed a total of 304 taxa across the three ecoregions, with 83 shared nodes (27.3%) and the Sandy Loam network containing the highest number of unique nodes (Fig. 4E).

Discussion

Research on *Ixodes* spp. ticks has demonstrated that various factors can influence tick microbiome composition. These factors include the host on which the tick has fed, geographical location, the tick's age, and its life stage [14, 38–40]. Studying the tick microbiome is of great interest, as it may help to understand pathogen colonization and transmission dynamics, and aids in developing effective control strategies [4]. In this study, we explored whether diverse ecological patterns influence microbial composition in ticks at the nymph life stage under natural conditions. We leveraged Belgium's unique topography, which extends from coastal plains to the Ardennes hills. Although a small country (~30,500 km²), Belgium is divided into 11 ecoregions,

each with distinct characteristics in vegetation, soil, and wildlife composition. Previous studies have demonstrated that the abundance and species composition of arthropods (e.g., isopods) vary depending on soil type and the different ecoregions in Belgium [41]. Here, we showed that significant differences exist across three very diverse ecoregions—Sandy Loam, Condroz, and Ardennes—in the prevalence of key pathogens and symbionts, as well as in sex distribution and microbial structure. Although prevalence data cannot be directly compared with other studies due to differences in nucleic acid extraction methodologies, the prevalence between ecoregions for each pathogen, symbiont, and sex ratio is comparable, as the same extraction method was used across all sites. In the Sandy Loam region, the proportion of males was significantly lower than in the two other ecoregions. Sandy Loam also had the highest prevalence of *S. ixodetis*-positive ticks. This is consistent with previous studies showing a higher prevalence of *S. ixodetis* in ticks collected from humans in Flanders compared to those from Wallonia [24]. *Spiroplasma* species have a male-killing effect on arthropods [42], which could explain the altered male-to-female ratio in this region, accounting for the lower number of male nymphs in Sandy Loam. Also, the prevalence of selected pathogens and symbionts across ecoregions demonstrated differences in tick microbiome composition. With the exception of *R. helvetica*, significant differences were observed for *B. burgdorferi* s.l., *A. phagocytophilum*, *Babesia* spp., and *N. mikurensis* across regions. Other studies have not observed these differences, but this discrepancy between our and the other studies may be related to differences in the source of collected ticks and the larger geographical dispersion of the study area [24] or the lower number of collected ticks [43]. Association networks computed using Yule's Q calculation revealed a positive association between *M. mitochondrii* and female nymphs in each ecoregion, while a negative interaction between this symbiont and male nymphs was observed. Studies have shown that *M. mitochondrii* is abundant in the mitochondria of female ticks, which explains the association between female nymphs and *M. mitochondrii* [44]. Interestingly, *M. mitochondrii* appeared to shape a distinct pathogenic pattern in two ecoregions. While associated with female ticks in all regions, it was in turn positively associated with *A. phagocytophilum* in Sandy Loam and with *B. burgdorferi* s.l. in the Ardennes. A positive association between *M. mitochondrii* and *B. burgdorferi* s.l. has been formerly reported. However, in the same study, the authors also found a negative association between *M. mitochondrii* and *A. phagocytophilum* [15]. As we did not observe the same microbial associations across the three ecoregions in Belgium, it is possible that the association of *M. mitochondrii* with *A. phagocytophilum* varies across regions and countries due to different geo-composition factors influencing the tick microbiome.

In Sandy Loam, *R. helvetica* was negatively correlated with *S. ixodetis*, which had a high prevalence in this region, suggesting a competitive interaction between these two microorganisms. Other studies also share these findings [15], indicating that ticks may not be able to maintain two symbiont species through vertical transmission, as they might compete with each other. Ticks' microbiome structure analysis showed that in *Rickettsia* positive ticks, *Spiroplasma* was significantly less abundant than in other ticks [13] confirming the competitive interaction between them.

Microbial structure derived from ONT analyses provided a deeper understanding of ecoregional differences and pathogen influences. Alpha diversity metrics showed that in both Sandy Loam and Condroz, higher observed features were found in *A. phagocytophilum* positive ticks in comparison with *R. helvetica* positive ticks, while in the Ardennes, observed features were higher in *S. ixodetis* positive ticks than in the three other microbe groups. Overall, taxa appeared to be less diverse in *R. helvetica* positive ticks compared to ticks infected with other microbes. Relative abundance analyses revealed three distinct microbial profiles for the ecoregions, further supported by beta dispersion analysis, which highlighted significant differences among them, with the Ardennes displaying a more heterogeneous microbial community. On the other hand, while the Jaccard distance again showed ecoregional clustering, this was not observed in ticks positive for *R. helvetica*, which clustered separately from the ecoregions. This suggests that the tick microbiome is similarly modulated by *R. helvetica* across all ecoregions. Therefore, tick microbiome composition appeared to be shaped by two factors: ecoregion and the presence of *R. helvetica*. The effects of *R. helvetica* on the tick microbiome have been studied by other groups, and their results clearly demonstrated that *R. helvetica* infection is associated with reduced bacterial diversity of the ticks microbiome [20]. A study on the presence of *Rickettsia* in ticks showed that when this taxa is removed in silico, the whole structure and function of the microbiome are altered [19]. These findings support the fact that *Rickettsia* shapes microbiome composition. A study performed in the Netherlands showed that the microbiome of *I. ricinus* ticks differed between distinct geographical locations [25]. In this study, authors demonstrate that the microbiomes of *I. ricinus* ticks changed depending on the area and that it changed gradually rather than randomly. In addition, the prevalence of symbionts (*R. helvetica*, *Rickettsiella* spp., *M. mitochondrii*, and *S. ixodetis*) in ticks differed between areas, confirming geographical variation in the ticks microbiome [25].

Some pathogen and symbionts detected by qPCR were not found in the taxonomic table after 16S rRNA ONT sequencing. This discrepancy was expected, since qPCR targets a single, highly conserved gene region with primers optimized for each pathogen or symbiont, whereas ONT

16S rRNA sequencing captures the full bacterial community through universal primers that may under-amplify low-abundance or primer-mismatched taxa. This complementary application of qPCR and untargeted 16S rRNA sequencing thus provides both high sensitivity for specific pathogens and a broad overview of community structure, underscoring the value of integrating targeted and untargeted approaches in tick-microbiome studies.

A methodological consideration in our study relates to the use of a minimal abundance filter of three reads per OTU following stringent contaminant removal using Decontam [30]. This approach was chosen to retain rare but potentially ecologically important taxa while minimizing the inclusion of sequencing artefacts [30]. Although some might argue that this cutoff is low, it reflects the growing recognition of the “rare biosphere” as a reservoir of genetic diversity and functional potential within microbial communities. Rare taxa, often excluded in more conservative filtering approaches, can play critical roles in community dynamics and may respond to environmental changes or perturbations [45]. Nevertheless, despite rigorous contaminant filtering, some low-level sequencing noise may persist, and thus, caution is warranted when interpreting the biological significance of very low-abundance OTUs. Future work incorporating technical replicates, complementary methods, or deeper sequencing depth would help to further validate the ecological relevance of these rare taxa. Overall, this filtering strategy enabled a more comprehensive characterization of the tick microbiome across diverse ecological regions.

Microbiome network analysis revealed differences between ecoregions, supporting again the shaping of the tick microbiome by the ecoregions. Sandy Loam network was more connected and more robust than the two others, indicating that taxa in this ecoregion interact with many others. On the other hand, the Sandy Loam network was completely different in pairwise comparison, and Condroz and Ardennes were sharing similar features. The shared modules (taxa) between Condroz and Ardennes also corresponded to the major modules in both networks. Local connectivity of microbes within the networks also shows that Sandy Loam was the most connected network as all four highly prevalent microbes (*Anaplasma*, *Borrelia*, *Rickettsia*, and *Spiroplasma*) were found. Interestingly, *Anaplasma* was present in the second largest module in Sandy Loam. Also, in the Ardennes, *Borrelia* was found to interact with *Candidatus Midichloria*, which corroborates findings observed with the qPCR association where *B. burgdorferi* s.l. was positively associated with *M. mitochondrii*.

While our study identifies clear geographic variation in microbiome composition, we did not directly assess vertebrate host communities. It is possible the variation in host identity, abundance, and feeding preferences across ecoregions could plausibly have driven differences in both

pathogen exposure and microbiome structure observed in this study. The regions considered in this study are indeed relatively biodiverse: the Ardennes is characterized by dense forests and supports a rich community of large mammals such as red deer, wild boar, and roe deer, as well as carnivores and small mammals [46]. The Condroz features a patchwork of woodlands and agricultural fields where roe deer are also found along with wild boar, carnivores, and smaller mammals [47]. The Sandy Loam region, with its sandy soils and more intensively managed landscapes, supports a community dominated by species like rodents and insectivores; it is also an important stopover site for migratory birds [48, 49]. As shown in other studies, differences in vertebrate hosts likely influence tick blood meal composition and, consequently, microbial community dynamics [40]. Thus, the distinct host communities across ecoregions likely contribute to the microbiome differences observed in this study.

In conclusion, our study reveals and confirms that the tick microbiome is shaped by the geographical and ecological characteristics of the location where the tick is collected. It also emphasizes the role of *R. helvetica* in contributing to microbiome modulation, as well as the possible influence of *S. ixodetis* on the sex ratio balance in specific regions. This is the first study on microbiome composition in Belgium, and it aims to enhance our understanding of regional differences in transmission dynamics of zoonotic pathogens.

Supplementary Information The online version contains supplementary material available at <https://doi.org/10.1007/s00248-025-02571-8>.

Acknowledgements We acknowledge the assistance of our colleagues in the laboratory, with special thanks to Martine Marin for her valuable technical support. The doctoral thesis of Camille Philippe and part of this work are supported by Sciensano through the internal VBDExpert project.

Author Contributions Conceptualization: M.M., C.P., H.S., A.C.C.; tick collection: C.P.; formal analysis: C.P. and M.F. (part of qPCR analyses); training and support in bioinformatics analysis: L.A.D., D.O., A.M., and S.S.; bioinformatics analysis: C.P.; supervision on bioinformatics analysis: A.C.C.; data curation: C.P., A.C.C. and M.M.; scientific and technical support: F.E.D., B.D. and E.C.; project administration, funding acquisition, and C.P. supervision: M.M.; writing—original draft preparation: C.P.; writing—review and editing: M.M. and A.C.C.; all authors revised and approved the final version of the manuscript.

Funding The doctoral thesis of Camille Philippe and part of this work are supported by Sciensano through the internal VBDExpert project.

Data Availability All data generated or analyzed during this study are included in this article and its supplementary information files. Raw sequence reads have been deposited in the Sequence Read Archive (SRA) public repository under the BioProject accession number PRJNA1236313.

Declarations

Competing Interests The authors declare no competing interests.

Open Access This article is licensed under a Creative Commons Attribution-NonCommercial-NoDerivatives 4.0 International License, which permits any non-commercial use, sharing, distribution and reproduction in any medium or format, as long as you give appropriate credit to the original author(s) and the source, provide a link to the Creative Commons licence, and indicate if you modified the licensed material. You do not have permission under this licence to share adapted material derived from this article or parts of it. The images or other third party material in this article are included in the article's Creative Commons licence, unless indicated otherwise in a credit line to the material. If material is not included in the article's Creative Commons licence and your intended use is not permitted by statutory regulation or exceeds the permitted use, you will need to obtain permission directly from the copyright holder. To view a copy of this licence, visit <http://creativecommons.org/licenses/by-nc-nd/4.0/>.

References

- de la Fuente J, Antunes S, Bonnet S et al (2017) Tick-pathogen interactions and vector competence: identification of molecular drivers for tick-borne diseases. *Front Cell Infect Microbiol* 7:114. <https://doi.org/10.3389/fcimb.2017.00114>
- Bonnet SI, Binetruy F, Hernández-Jarguín AM, Duron O (2017) The tick microbiome: why non-pathogenic microorganisms matter in tick biology and pathogen transmission. *Front Cell Infect Microbiol* 7:236. <https://doi.org/10.3389/fcimb.2017.00236>
- Hussain S, Perveen N, Hussain A et al (2022) The symbiotic continuum within ticks: opportunities for disease control. *Front Microbiol* 13:854803. <https://doi.org/10.3389/fmicb.2022.854803>
- Wu-Chuang A, Hodžić A, Mateos-Hernández L et al (2021) Current debates and advances in tick microbiome research. *Curr Res Parasitol Vector-Borne Dis* 1:100036. <https://doi.org/10.1016/j.crpvbd.2021.100036>
- Duron O (2024) Nutritional symbiosis in ticks: singularities of the genus *Ixodes*. *Trends Parasitol* 40:696–706. <https://doi.org/10.1016/j.pt.2024.06.006>
- Narasimhan S, Rajeevan N, Liu L et al (2014) Gut microbiota of the tick vector *Ixodes scapularis* modulate colonization of the Lyme disease spirochete. *Cell Host Microbe* 15:58–71. <https://doi.org/10.1016/j.chom.2013.12.001>
- Abuin-Denis L, Piloto-Sardiñas E, Maitre A et al (2024) Exploring the impact of *Anaplasma phagocytophilum* on colonization resistance of *Ixodes scapularis* microbiota using network node manipulation. *Curr Res Parasitol Vector Borne Dis* 5:100177. <https://doi.org/10.1016/j.crpvbd.2024.100177>
- Wu-Chuang A, Mateos-Hernandez L, Maitre A et al (2023) Microbiota perturbation by anti-microbiota vaccine reduces the colonization of *Borrelia afzelii* in *Ixodes ricinus*. *Microbiome* 11:151. <https://doi.org/10.1186/s40168-023-01599-7>
- Maldonado-Ruiz P (2024) The tick microbiome: the “other bacterial players” in tick biocontrol. *Microorganisms* 12:2451. <https://doi.org/10.3390/microorganisms12122451>
- Thapa S, Zhang Y, Allen MS (2018) Effects of temperature on bacterial microbiome composition in *Ixodes scapularis* ticks. *Microbiologypopen* 8:e00719. <https://doi.org/10.1002/mbo3.719>
- Wu-Chuang A, Obregon D, Estrada-Peña A, Cabezas-Cruz A (2022) Thermostable keystone bacteria maintain the functional diversity of the *Ixodes scapularis* microbiome under heat stress. *Microb Ecol* 84:1224–1235. <https://doi.org/10.1007/s00248-021-01929-y>
- Abraham NM, Liu L, Jutras BL et al (2017) Pathogen-mediated manipulation of arthropod microbiota to promote infection. *Proc Natl Acad Sci U S A* 114:E781–E790. <https://doi.org/10.1073/pnas.1613422114>
- Lejal E, Chiquet J, Aubert J et al (2021) Temporal patterns in *Ixodes ricinus* microbial communities: an insight into tick-borne microbe interactions. *Microbiome* 9:153. <https://doi.org/10.1186/s40168-021-01051-8>
- Swei A, Kwan JY (2017) Tick microbiome and pathogen acquisition altered by host blood meal. *ISME J* 11:813–816. <https://doi.org/10.1038/ismej.2016.152>
- Krawczyk AI, Röttgers S, Coimbra-Dores MJ et al (2022) Tick microbial associations at the crossroad of horizontal and vertical transmission pathways. *Parasit Vectors* 15:380. <https://doi.org/10.1186/s13071-022-05519-w>
- Hodosi R, Kazimirova M, Soltys K (2022) What do we know about the microbiome of *I. ricinus*? *Front Cell Infect Microbiol* 12:. <https://doi.org/10.3389/fcimb.2022.990889>
- Aivelo T, Lemoine M, Tschirren B (2022) Elevational changes in bacterial microbiota structure and diversity in an arthropod-disease vector. *Microb Ecol* 84:868–878. <https://doi.org/10.1007/s00248-021-01879-5>
- Van Treuren W, Ponnusamy L, Brinkerhoff RJ et al (2015) Variation in the microbiota of *Ixodes* ticks with regard to geography, species, and sex. *Appl Environ Microbiol* 81:6200–6209. <https://doi.org/10.1128/AEM.01562-15>
- Maitre A, Wu-Chuang A, Mateos-Hernández L et al (2023) Rickettsial pathogens drive microbiota assembly in *Hyalomma marginatum* and *Rhipicephalus bursa* ticks. *Mol Ecol* 32:4660–4676. <https://doi.org/10.1111/mec.17058>
- Maitre A, Wu-Chuang A, Mateos-Hernández L et al (2022) *Rickettsia helvetica* infection is associated with microbiome modulation in *Ixodes ricinus* collected from humans in Serbia. *Sci Rep* 12:11464. <https://doi.org/10.1038/s41598-022-15681-x>
- Belgium | Biodiversity Information System for Europe. <https://biodiversity.europa.eu/countries/belgium>. Accessed 27 Feb 2025
- Brognia D, Dufrêne M, Michez A et al (2018) Forest cover correlates with good biological water quality. Insights from a regional study (Wallonia, Belgium). *J Environ Manage* 211:9–21. <https://doi.org/10.1016/j.jenvman.2018.01.017>
- Drossart et al (2019) Belgian red list of bees.pdf. <https://www.natuurpunt.be/publicaties/belgian-red-list-of-bees-2019>. Accessed 27 Feb 2025
- Philippe C, Geebelen L, Hermy MRG et al (2024) The prevalence of pathogens in ticks collected from humans in Belgium, 2021, versus 2017. *Parasit Vectors* 17:380. <https://doi.org/10.1186/s13071-024-06427-x>
- Krawczyk AI, Röttgers L, Fonville M et al (2022) Quantitative microbial population study reveals geographical differences in bacterial symbionts of *Ixodes ricinus*. *Microbiome* 10:120. <https://doi.org/10.1186/s40168-022-01276-1>
- Köhler CF, Holding ML, Fonville M et al (2025) *Midichloria mitochondrii* stimulates the sylvatic cycle of *Borrelia burgdorferi* (*sensu lato*) in *Ixodes ricinus* and contributes to Lyme disease risk. *Curr Res Parasitol Vector Borne Dis* 8:100290. <https://doi.org/10.1016/j.crpvbd.2025.100290>
- Quast C, Pruesse E, Yilmaz P et al (2013) The SILVA ribosomal RNA gene database project: improved data processing and web-based tools. *Nucleic Acids Res* 41:D590–596. <https://doi.org/10.1093/nar/gks1219>
- Edwards U, Rogall T, Blöcker H et al (1989) Isolation and direct complete nucleotide determination of entire genes. Characterization of a gene coding for 16S ribosomal RNA. *Nucleic Acids Res* 17:7843–7853
- R Core Team (2021) R: a language and environment for statistical computing. R Foundation for Statistical Computing, Vienna, Austria. URL <https://www.R-project.org/>. Accessed 27 Feb 2025

30. Davis NM, Proctor DM, Holmes SP et al (2018) Simple statistical identification and removal of contaminant sequences in marker-gene and metagenomics data. Microbiome 6:226. <https://doi.org/10.1186/s40168-018-0605-2>
 31. Oksanen J, Simpson GL, Blanchet FG, Kindt R, Legendre P, Minchin PR et al Vegan: community ecology package. Version 2.6–10. <https://cran.r-project.org/web/packages/vegan/vegan.pdf>. Accessed 27 Feb 2025
 32. Fernandes AD, Macklaim JM, Linn TG et al (2013) ANOVA-like differential expression (ALDEx) analysis for mixed population RNA-Seq. PLoS ONE 8:e67019. <https://doi.org/10.1371/journal.pone.0067019>
 33. Inferring correlation networks from genomic survey data | PLOS Computational Biology. <https://doi.org/10.1371/journal.pcbi.1002687>. Accessed 27 Feb 2025
 34. Abuin-Denis L, Piloto-Sardiñas E, Maitre A et al (2024) Differential nested patterns of *Anaplasma marginale* and *Coxiella*-like endosymbiont across *Rhipicephalus microplus* ontogeny. Microbiol Res 286: 127790. <https://doi.org/10.1016/j.micres.2024.127790>
 35. Peschel S, Müller CL, von Mutius E et al (2020) NetComi: network construction and comparison for microbiome data in R. Brief Bioinform 22:bbaa290. <https://doi.org/10.1093/bib/bbaa290>
 36. Lhomme S (2015) Analyse spatiale de la structure des réseaux techniques dans un contexte de risques. Cybergeog 2015:711. <https://doi.org/10.4000/cybergeog.26763>
 37. Freitas S, Yang D, Kumar S, et al (2021) Evaluating graph vulnerability and robustness using TIGER. <https://doi.org/10.1145/3459637.3482002>
 38. Zhang X-C, Yang Z-N, Lu B et al (2014) The composition and transmission of microbiome in hard tick, *Ixodes persulcatus*, during blood meal. Ticks Tick Borne Dis 5:864–870. <https://doi.org/10.1016/j.ttbdis.2014.07.009>
 39. Daveu R, Laurence C, Bouju-Albert A et al (2021) Symbiont dynamics during the blood meal of *Ixodes ricinus* nymphs differ according to their sex. Ticks Tick Borne Dis 12:101707. <https://doi.org/10.1016/j.ttbdis.2021.101707>
 40. Landesman WJ, Mulder K, Allan BF et al (2019) Potential effects of blood meal host on bacterial community composition in *Ixodes scapularis* nymphs. Ticks Tick Borne Dis 10:523–527. <https://doi.org/10.1016/j.ttbdis.2019.01.002>
 41. Boeraeve P, Arijs G, Segers S et al (2022) Inventory of the terrestrial isopods in Belgium (2011–2020). ZooKeys 1101:57–69. <https://doi.org/10.3897/zookeys.1101.65810>
 42. Arai H, Inoue MN, Kageyama D (2022) Male-killing mechanisms vary between Spiroplasma species. Front Microbiol 13:1075199. <https://doi.org/10.3389/fmicb.2022.1075199>
 43. Adjadj NR, Cargnel M, Ribbens S et al (2023) Prevalence of Anaplasma phagocytophilum, Borrelia burgdorferi sensu lato, Rickettsia spp. and Babesia spp. in cattle serum and questing ticks from Belgium. Ticks and Tick-borne Diseases 14:102146. <https://doi.org/10.1016/j.ttbdis.2023.102146>
 44. Epis S, Mandrioli M, Genchi M et al (2013) Localization of the bacterial symbiont Candidatus Midichloria mitochondrii within the hard tick Ixodes ricinus by whole-mount FISH staining. Ticks Tick Borne Dis 4:39–45. <https://doi.org/10.1016/j.ttbdis.2012.06.005>
 45. Sogin ML, Morrison HG, Huber JA et al (2006) Microbial diversity in the deep sea and the underexplored “rare biosphere.” Proc Natl Acad Sci U S A 103:12115–12120. <https://doi.org/10.1073/pnas.0605127103>
 46. Belgium Biodiversity and Nature Conservation | BioDB. <https://biodb.com/region/belgium/>. Accessed 11 Jun 2025
 47. Défi Nature. <https://defi-nature.be/blog/le-condroz>. Accessed 11 Jun 2025
 48. Régions biogéographiques en Belgique. In: Biologie végétale. <https://biologievegetale.be/ecologie-vegetale/ecosystemes/phytogeographie/regions-biogeographiques-en-belgique/>. Accessed 11 Jun 2025
 49. Vizuality Belgium Interactive Forest Map & Tree Cover Change Data | GFW. <https://www.globalforestwatch.org/map/chapter/BEL/?map=eyJjZW50ZXIiOiNpbGF0Ijo1MC40NDg5MTEzOTYzMjA4NCwibG5nIjo0LjgyMjQ0OTc4NzZmNDM5N30sInpvb20iOjYuOTIzNTI3MTIzMTEiODg2LCJkYXRhc2V0ciJlW3siZGF0YXNldCI6ImxhbmQtY292ZXIlLCJvcGFjaXR5Ijo1LCJ2aXNpYmlsaXR5Ijp0cnVILCJsYXllcnMiOlslbGFuZCJlb3ZlcioyMDE1III9LHsiZGF0YXNldCI6ImBvbGl0aWNhbC1ib3VuZGFyaWVzIiwibG9saXRpY2FzLWJvdW5kYXJpZXMiXSwib3BhY2I0eSI6MSwidmIzazWjbG10eSI6dHJ1ZXIldfQ%3D%3D&mapMenu=eyJjZW51U2VjdGlvbil6ImRhdGFzZXRxziwiZGF0YXNldENhdGVnb3J5IjoibGFuZENvdmVyIn0%3D&mapPrompts=eyJjZdGVwc0tleSI6ImFuYWx5emVBbkFyZWEiLCJzdGVwc0luZGV4IjowLCJmb3JzJSI6dHJ1ZX0%3D>. Accessed 11 Jun 2025
- Publisher's Note** Springer Nature remains neutral with regard to jurisdictional claims in published maps and institutional affiliations.

Publisher's Note Springer Nature remains neutral with regard to jurisdictional claims in published maps and institutional affiliations.